TRANSIENT BEHAVIOR OF ELECTRORHEOLOGICAL FLUIDS IN SHEAR FLOW

DAVID KITTIPOOMWONG AND DANIEL J. KLINGENBERG

Department of Chemical and Biological Engineering and Rheology Research Center, University of Wisconsin, 1415 Engineering Dr., Madison, WI 53706, USA

E-mail: klingen@engr.wisc.edu

JEFFREY F. MORRIS

Levich Institute and Department of Chemical Engineering, City College of New York, New York, NY

Email: morris@ccny.cuny.edu

The transient response of electrorheological suspensions in shear flow subjected to a suddenly imposed electric field is investigated experimentally. Barium titanate/silicone oil and alumina/mineral oil suspensions are employed. The evolution of both the rheological properties and suspension structure are investigated. Transient responses appear above a critical field field strength, and the critical Mason number for the onset of a transient rheological response is equivalent to the critical Mason number for the onset of lamella formation, within experimental uncertainty. These results are consistent with previous predictions. However, the shear rate and volume fraction dependence of the critical Mason number deviate from that predicted.

1 Introduction

Electrorheological (ER) and magnetorheological (MR) suspensions exhibit dramatic changes in rheological properties upon the application of electric or magnetic fields, respectively. The suspensions change from viscous liquids to viscoplastic solids in the order of milliseconds.[1,2,3] The dramatic rheological changes are closely associated with a change in microstructure. At zero field strength, the microstructure is isotropic. Upon the application of the external field, the particles aggregate into columnar structures. The rapid initial increase in apparent viscosity caused by the applied field can be followed by a much slower transient increase in the apparent viscosity.[4,5] Such behavior is believed to be intimately connected to the field-induced formation of lamellar structures in shear flow.[4,5,6,7,8]

von Pfeil et al.[9] examined the shear-induced structure in ER and MR suspensions by employing a two-fluid continuum model. The evolution of the particle concentration is governed by the competition of field-induced and hydrodynamic particle stresses. The resulting conservation equation for the particle volume fraction yields column-like structures in quiescent suspensions and lamellar structures in shear flow, consistent with experimental observations. Employing a linear stability analysis, the authors predicted three features of the structure evolution under shear that are relevant to this article: (1) lamellar structures should appear only for field strengths greater than a critical field strength, E_c; (2) the critical field strength corresponds to a critical Mason number, $\mathrm{Mn}_c = \eta_c\dot{\gamma}/(2\epsilon_0\epsilon_c\beta^2 E_c^2)$, which should be independent of shear rate, but depends on the particle concentration. Here, η_c is the suspending fluid viscosity, $\dot{\gamma}$ is the shear rate, $\epsilon_0 = 8.8542 \times 10^{-12}$ F/m, ϵ_c is the relative dielectric constant of the the suspending fluid, and β is the relative particle polarizability;[10] and (3) the predicted dependence of Mn_c on the volume fraction is of a specific form, $\mathrm{Mn}_c = 2\phi_{\max}^2 \left(1 - \phi/\phi_{\max}\right)^3 / \left(1 - \beta\phi\right)^3$, where ϕ is the particle volume fraction and $\phi_{\max}$ is the maximum packing fraction. Although these predictions pertain to the evolution of the microstructure, it follows that a transient structure evolution should give rise to a transient rheological response.[11]

Ulicny et al.[5] investigated the transient rheological response of MR suspensions composed of carbonyl iron particles in an aliphatic oil. Fumed silica was added to slow sedimentation; the fumed silica also imparted non-Newtonian character to the suspension in the absence of a magnetic field. For small field strengths, the apparent suspension viscosity rapidly increased to a steady value when the field was applied. However, for sufficiently large field strengths, a transient shear stress was observed. The appearance of a transient response for field strengths above a critical value is consistent with the first prediction described in the previous paragraph. However, Ulicny et al. found that the critical Mason number increased substantially with shear rate, and the values were much smaller than those predicted by von Pfeil et al. The authors attributed the discrepancies between their experimental observations and the predictions in part to effects of the colloidal forces imparted by the fumed silica, which are not considered in the continuum model.

In this report, we describe an experimental investigation of the transient rheological response and microstructure evolution in ER suspensions in shear flow. The rheological response to a suddenly imposed electric field only exhibits a slow transient above a critical field strength, in agreement with the predictions of von Pfeil et al.[9] Experiments in which the rheological and structural responses are monitored simultaneously reveal that the critical Mason numbers marking the onset of a transient rheological response and the appearance of lamellar structures are equivalent within experimental uncertainty. However, the shear rate and volume fraction dependence of the critical Mason number differ from that predicted.

2 Experimental

Alumina suspensions were composed of acidic alumina particles (Al_2O_3) in heavy mineral oil (viscosity $\eta_c = 0.198$ Pa·s) with Brij®30 as a surfactant. The amount of surfactant was 2.5 wt% (based on the particle mass). Barium titanate suspensions were composed of barium titanate particles ($BaTiO_3$) in silicone oil (viscosity $\eta_c = 0.504$ Pa·s) with no surfactant added. Both the alumina and the barium titanate particles were ground with a mortar and pestle and sieved to obtain particle diameters in the range 53–90 μm. The particles were dried for 12 hours at 110 °C. The oils were stored over molecular sieves overnight to remove water.

Rheological measurements were made using a Bohlin VOR rheometer configured with either parallel disk or concentric cylinder geometries. The stainless steel parallel disks are attached to Delrin fixtures to electrically insulate the disks from the rheometer. A potential difference is applied across the disks using a Trek 10/10 amplifier driven with a function generator, connected to the top plate with a wire, and to the bottom plate with a sliding contact. The concentric cylinder cell is composed of a stainless steel bob and transparent quartz cup, each connected to Delrin fixtures. The inner surface of the cup was made electrically conducting with a coating of indium tin oxide.[12] For all experiments reported here, ac electric fields are employed, with frequencies of 300 Hz for alumina suspensions, and 500 Hz for barium titanate suspensions.

Rheological experiments were performed as follows. Suspensions were first sheared at a large shear rate ($\dot{\gamma} \geq 50\ s^{-1}$) with no applied field to ensure that the particles were

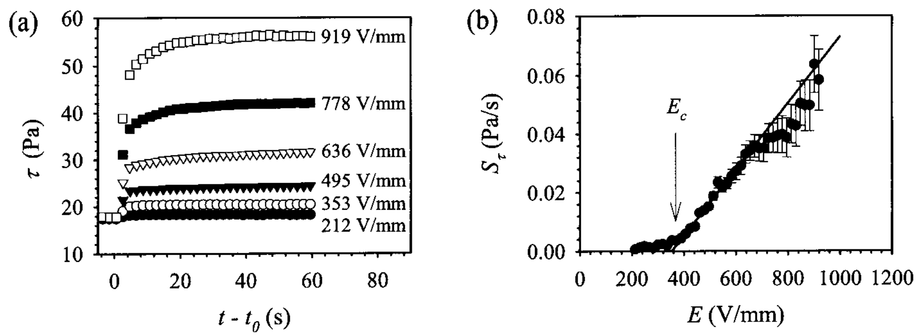

Figure 1. (a) Shear stress of 12.8 vol% barium titanate suspensions as a function of time for different applied field strengths ($\dot{\gamma} = 19.9\ s^{-1}$). (b) Slope of shear stress vs time as a function of field strength for 12.8 vol% barium titanate suspensions ($\dot{\gamma} = 19.9\ s^{-1}$).

distributed homogeneously. The shear rate was then set to the desired value and maintained for 30 s with no applied field. An electric field was then applied for 1-3 minutes. The field strength was then set to zero and the shear stress was recorded for another 30 seconds. These measurements were repeated for various field strengths, shear rates and concentrations. All experiments were carried out at room temperature (20–25°C).

The evolution of the suspension structure in the concentric cylinder geometry was examined by recording video images with a CCD video camera. The camera was directed normal to the outer transparent cylinder. Video images were analyzed using NIH image processing software. Raw images were sharpened using an FFT filter.

3 Results

The shear stress τ of a 12.8 vol% barium titanate suspension is plotted in Fig. 1(a) as a function of time after the electric field has been applied, $t - t_0$, for various field strengths (parallel disks; $\dot{\gamma} = 19.9 s^{-1}$). When the field is applied, the shear stress initially increases rapidly, as commonly observed in ER fluids. For sufficiently large field strengths, the stress then continues to increase slowly.

Following Ulicny et al.,[5] we characterize the slow transient rheological response by the slope S_τ of the shear stress vs time data, while the field is applied. This slope is calculated by linear regression of the data collected over the period $2 < t - t_0 < 60$ s; data collected during the first two seconds after the field is applied are ignored in order to avoid potential problems with a lag in the data acquisition. The slope is plotted as a function of electric field strength in Fig. 1(b) for 12.8 vol% barium titanate suspensions at $\dot{\gamma} = 19.9\ s^{-1}$. There is a clear transition in the behavior of the shear stress. For small E, S_τ is indistinguishable from zero, which indicates steady shear flow. For sufficiently large E, $S_\tau > 0$, which indicates a transient increase in the shear stress.

We define a critical field strength, E_c, as the field strength at which slope begins to deviate from zero. The value of E_c is obtained by linear regression of the data for which $S_\tau > 0$, equating E_c with the intercept on the abscissa as illustrated in Fig. 1(b). Data for all runs were analyzed in this manner. The critical field strength corresponds to a critical

Mason number $\mathrm{Mn}_c = \eta_c \dot{\gamma}/(2\epsilon_0 \epsilon_c \beta^2 E_c^2)$, which is plotted as a function of $\dot{\gamma}$ for the barium titanate and alumina suspensions at various concentrations in Fig. 2 (using $\epsilon_c = 2$ and $\beta = 1$). For some of the systems represented in Fig. 2, Mn_c does not vary with $\dot{\gamma}$ within experimental uncertainty; for other systems, Mn_c increases with $\dot{\gamma}$ by an amount comparable with the experimental uncertainty. We thus conclude that Mn_c depends, at most, weakly on shear rate. This differs from that predicted by von Pfeil et al.[9] where Mn_c is independent of shear rate. We note that Ulicny et al.[5] reported that Mn_c increased significantly with shear rate for MR suspensions composed of iron and fumed silica particles in an aliphatic oil.

Next, we consider the behavior of alumina suspensions in shear flow between concentric cylinders. The outer cylinder is transparent so that the evolution of the suspension structure could be observed simultaneously with the rheological measurements. Video images for shear flow of an alumina suspension ($\phi = 0.15$, $\dot{\gamma} = 29.2\ \mathrm{s}^{-1}$) at various field strengths and times are presented in Fig. 3, where the motion of the outer cylinder is from left to right. For sufficiently small electric field strengths, suspensions under shear appear to be homogeneous, with no variation of the particle concentration along the axial direction. For large field strengths, lamellar patterns oriented in the flow direction form after the field is applied.

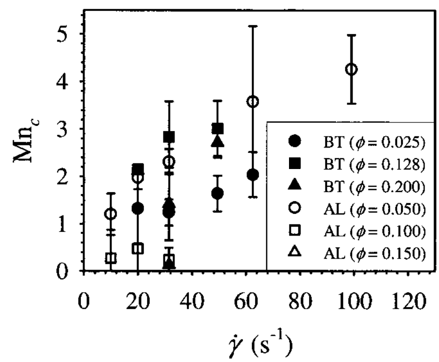

Figure 2. Critical Mason number as a function of shear rate for barium titanate (BT) and alumina (AL) suspensions at different concentrations.

The suspension structure evolves slowly with time, as the lamella coalesce into larger lamella. This is illustrated in Fig. 4(a) where the average stripe thickness h is plotted as a function of time after the application of the electric field for a 15 vol% alumina suspension ($\dot{\gamma} = 29.2\ \mathrm{s}^{-1}$). At a field strength of 612 V/mm, lamella do not form; this is represented in Fig. 4(a) by the symbols at $h = 0$. The large error bars in Fig. 4(a) characterize the variation in lamella thickness throughout the gap, which is also apparent in Fig. 3.

The transient evolution of the lamellar patterns is characterized similarly to the rheological response, via the slope $S_h \equiv dh/dt$, obtained by linear regression of the data $h(t)$ for $2 < t < 180$ s. The slope S_h is plotted as a function of electric field strength in Fig. 4(b) for a 15 vol% suspension of alumina particles ($\dot{\gamma} = 29.2\ \mathrm{s}^{-1}$). Also plotted is the slope S_τ of the transient shear stress. These two measures of transient responses exhibit similar behavior, and similar to that depicted in Fig. 1(b). For small field strengths, the rates of change are indistinguishable from zero (and lamella are not present), while for large field strengths, transient behavior arises.

It is apparent in Fig. 4(b) that the onset of lamella formation occurs at roughly the same field strength as the onset of a transient rheological response, supporting the notion that the transient rheological response is caused by lamella formation. The critical field strengths for the onset of transient behavior are compared quantitatively for alumina sus-

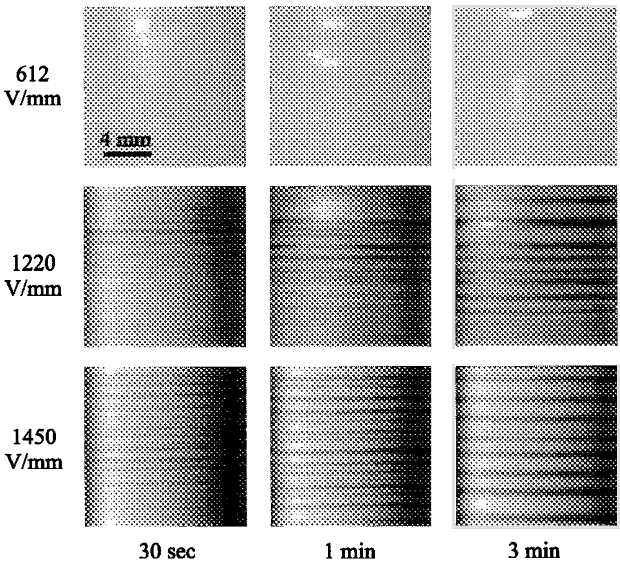

Figure 3. Suspension structure as a function of time for 15 vol% alumina suspensions at various field strengths ($\dot{\gamma} = 29.2\,\mathrm{s}^{-1}$).

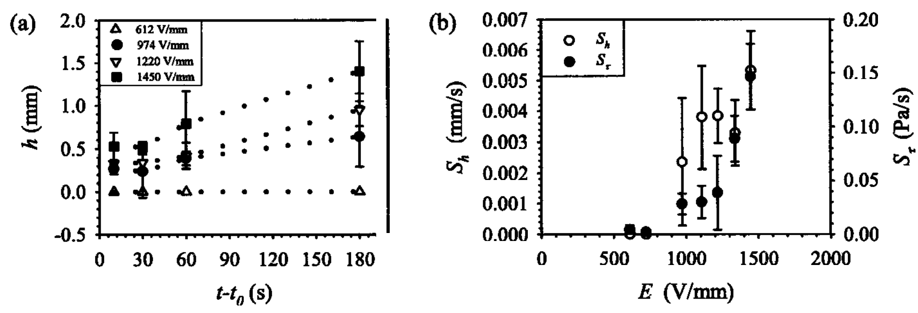

Figure 4. (a) Average stripe thickness as a function of time for 15 vol% alumina suspensions at various field strengths ($\dot{\gamma} = 29.2\,\mathrm{s}^{-1}$). (b) Rates of change of average lamellae thickness (S_h) and shear stress (S_τ) as functions of applied field strength for 15 vol% alumina suspensions ($\dot{\gamma} = 29.2\,\mathrm{s}^{-1}$).

pensions at various concentrations ($\dot{\gamma} = 29.2\,\mathrm{s}^{-1}$) in Table 1. Again, the critical field strengths obtained from rheological and microstructural data agree reasonably well for all concentrations.

In Fig. 5, Mn_c is plotted as a function of concentration for alumina and barium titanate suspensions. The values of Mn_c in this figure were obtained by averaging the results obtained from rheological experiments at different shear rates. For alumina suspensions, results from experiments with both parallel disk and concentric cylinder geometries are included. Also plotted in Fig. 5 is the prediction reported by von Pfeil et al.[9] There are several features to point out in this figure. First, the experimental results are closer to that

Table 1. Critical field strength as a function of concentration for alumina suspensions ($\dot{\gamma} = 29.2\ \mathrm{s}^{-1}$).

ϕ	E_c (V/mm)	
	rheological data	image analysis
0.05	448 ± 44	442 ± 69
0.10	837 ± 106	786 ± 80
0.15	1172 ± 165	1058 ± 114

predicted than the experimental results reported for MR suspensions by Ulicny et al., where $2 \times 10^{-5} < \mathrm{Mn} < 5 \times 10^{-3}$.[5] Second, results for alumina suspensions using different geometries agree within experimental uncertainty. Finally, the experimental results exhibit a dependence of $\mathrm{Mn}_c(\phi)$ on particle type. For barium titanate suspensions, Mn_c increases with concentration initially. For alumina suspensions, Mn_c decreases monotonically with increasing concentration. The experimental results for different particle types only appear to be similar, and similar to that predicted, at small concentrations.

There are several possible explanations for the different values of Mn_c obtained for different materials, which does not seem to be captured by the continuum model. First, Ulicny et al.[5] suggested that colloidal forces may significantly influence the value of Mn_c. We have made no attempt to characterize the colloidal forces for our systems. Second, in the continuum analysis described by von Pfeil et al.,[9] a point-dipole model was employed for the electrostatic stresses. This model approximately captures the many-body electrostatic interactions between particles, producing a dependence of Mn_c on particle type through its dependence on the relative polarizability β (see Sec. 1). However, since we expect β to be near one for both particle types [e.g., for barium titanate, $\epsilon \approx 2000$ at large frequencies, which gives $\beta \approx 0.996$ for silicone oil with dielectric constant $\epsilon_c = 2.75$.[13,14] For alumina particles in silicone oil at $\phi = 0.057$ with 3 wt% Brij®30, Kim reported a dielectric constant at 300 Hz of 3.77[15]; the suspension dielectric constant obtained from Maxwell's formula $\epsilon = \epsilon_c(1 + 2\beta\phi)/(1 - \beta\phi)$ is 3.40 for $\beta = 1$, $\epsilon_c = 2.88$, suggesting that the actual value of β is near 1.0], this dependence is too weak to explain the experimental observations. It is well known that higher-order multipole interactions which were neglected in the continuum model can significantly affect field-induced forces, especially as $\beta \rightarrow 1$.[16] Inclusion of higher-order multipoles should therefore affect the suspension stress, and thus cause the critical Mason number to depend more sensitively on the materials' dielectric properties than predicted by the continuum model of von Pfeil et al.

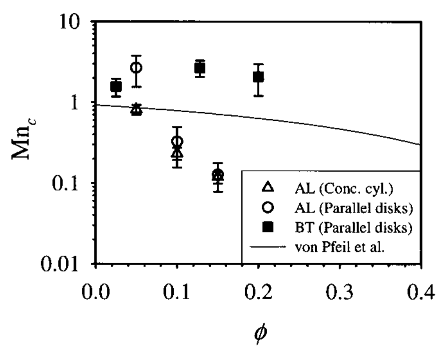

Figure 5. Critical Mason number as a function of particle volume fraction for barium titanate (BT) and alumina (AL) suspensions.

4 Conclusion

Experimental data for the transient evolution of the rheological properties and the structure of ER suspensions support the hypothesis that a transient rheological response is caused by the formation of lamella. Critical field strengths for onset of transient behavior are similar for both types of experiments. That transient behavior only appears above a critical field strength is consistent with the continuum model of von Pfeil et al.[9] However, the critical Mason number appears to depend weakly on shear rate, whereas von Pfeil et al. predict that the critical Mason number should be independent of shear rate. We also find that the volume fraction dependence of Mn_c differs from that predicted by von Pfeil et al., and different dependences are obtained for the alumina and barium titanate suspensions.

Acknowledgments

The authors thank D. Nest, L. Hsiao and J. Schmidt for helping with the experiments. This work was supported in part by the National Science Foundation under grant CTS-0424087, and by General Motors.

References

1. Tanaka, K., A. Sahashi, R. Akiyama and K.Koyama, Phys. Rev. E., **52**, 3325 (1995).
2. Nava, R., M. A. Ponce, L. Rejón, S. Viquez and V. M. Castano, Smart Mater. Struct., **6**, 67 (1997).
3. Tian, Y., C. Li, M. Zhang, Y. Meng and S. Wen, J. Coll. Int. Sci., **288**, 290 (2005).
4. Vieira, S. L., L. B. P. Neto and A. C. F. Arruda, J. Rheol., **44**, 1139 (2000).
5. Ulicny, J. C., M. A. Golden, C. S. Nanuduri and D. J. Klingenberg, J. Rheol., **49**, 87 (2005).
6. Henley, S. and F. E. Filisko, J. Rheol., **43**, 1323 (1999).
7. Tang, X., W. H. Li, X. J. Wang and P. Q. Zhang, Int. J. Mod. Phys. B, **13**, 1806 (1999).
8. Volkova, O., S. Cutillas and G. Bossis, Phys. Rev. Lett., **82**, 233 (1999).
9. von Pfeil, K., M. D. Graham, D. J. Klingenberg and J. F. Morris, J. Appl. Phys., **93**, 5769 (2003).
10. Parthasarathy, M. and D. J. Klingenberg, Mat. Sci. Eng. R, **R17**, 57 (1996).
11. von Pfeil, K., M.S. Thesis, University of Wisconsin, Madison, WI (2002).
12. Liu, J., E. Radlein and G. H. Frischat, Phys. Chem. Glasses, **40**, 277 (1999).
13. Rankin, P. J. and D. J. Klingenberg, J. Rheol., **42**, 639 (1998).
14. Lan, Y. C., S. Q. Men, X. Y. Xu and K. Q. Lu, J. Phys. D: Appl. Phys., **33**, 1239 (2000).
15. Kim, Y., Ph.D. thesis, University of Wisconsin, Madison, WI (1996).
16. Clercx, H. J. H. and G. Bossis, Phys. Rev. E., **48**, 2721 (1993).